BASALT FIBER WITH PYROLYTIC CARBON COATING FOR SENSORY APPLICATIONS

Bin Hao, Peng-Cheng Ma *

[1] Laboratory of Environmental Science and Technology, The Xinjiang Technical Institute of Physics and Chemistry, Key Laboratory of Functional Materials and Devices for Special Environments, Chinese Academy of Sciences, Urumqi 830011, China.

* Corresponding author. Tel: +86-991-6992225; E-mail: mapc@ms.xjb.ac.cn.

Keywords: Basalt fiber; Pyrolytic carbon coating; Fiber reinforced polymers; Pizeoresistive effect; Sensor

ABSTRACT

This paper reported the modification of basalt fiber (BF) using a chemical vapor deposition (CVD) method, aiming at rectifying the functionality of BF for sensory application. Various techniques were employed to characterize the surface, electrical and mechanical properties of fibers before and after CVD treatment. The results showed that a thin layer of pyrolytic carbon with thickness of 15-30 nm was coated on fiber surface, making the insulating fibers electrically conductive. When embedding a bundle of fibers into epoxy, the corresponding composites showed a piezoresistive effects with the largest gauge factor of 38.6 under the mechanical load. The analysis on stress-strain curve along with corresponding electrical resistance of sample confirmed that BF with pyrolytic carbon coating could be used as both reinforcement and sensor to monitor structural damage in composite structures.

1. INTRODUCTION

Basalt fiber (BF), a material made from extremely fine fiber of volcanic rock, has attracted much interest in recent years due to its low water absorption, marginal hazardness to health, excellent tolerance to temperature and environmental factors in comparison with glass fiber, as well as simplified process for scale-up production and much lower price when compared with carbon fiber [1]. Such unique advantages endow BF a suitable candidate for various applications, such as reinforcement for fiber reinforced polymers (FRPs) [2], fire structural resistance [3], thermal insulation material for concrete [4], and so on.

In contrast to the numerous studies on glass and carbon fibers, relatively few studies were reported on enhancing the functionality of BF. With rapid development of nanotechnology, the deposition/growth of carbon-based nanoparticles, such as carbon nanotubes (CNTs) and graphene, onto fiber surface, has become one of the common methods to functionalize traditional fibers [5, 6]. Such treatment not only improved the interphase strength between fiber and polymer matrix, but also turned insulating glass fiber to the electrically conductive one, thus extending the application of glass fiber into the areas like monitoring health state in FRP structures [6, 7], being a strain sensor [6, 7]. The process of depositing nanoparticles onto fiber surface can be accomplished by sizing, spray coating, dip coating and electrophoretic deposition [5, 7]. While the operation of these methods was simple, the fine controlling on the homogeneous thickness and surface properties of coating on fiber surface is a great challenge [5].

Pyrolytic carbon coating, a method producing crystallized graphite by heating a hydrocarbon nearly to its decomposition temperature, has been employed over the years to alumina, SiC, optical and carbon fibers to tailor the properties like improving hermetic properties of fibers [8], rectifying the microwave absorbing capability of composites [9], modifying the interfacial bonding between the fiber and matrix [10], facilitating the diffusivity of metal element in the coating [11]. Generally, pyrolytic carbon can be coated onto substrates which are stable at high temperature. In this context, the deposition of such carbon onto thermally stable BF may provide an alternative to enhancing the technical value of fiber. It should be noted that this kind of coating commonly consisted of ordered and disordered carbon nanostructures in the presence of turbo-stratic/rough laminar structure, making it possible to rectify the electrical properties of BF. In addition, the thickness of coating can be easily modulated to nano-scale by gas flow and operating time [12], providing a way to get a homogeneous surface coating for BF.

Motivated by the above discussion, we used a chemical vapor deposition (CVD) process to deposit pyrolytic carbon coating onto BF, aiming at endowing BF with multi-functionalities. The effect of coating on the mechanical and electrical properties of BF was studied, and the application of modified fiber as strain sensor in FRP structure was also explored.

2. EXPERIMENTAL

2.1 PREPARATION OF SAMPLES

BF with an average diameter of 15.0 μm and fineness of 100 tex (Asamer Basaltic Fibers GmbH) was used in this study. Fig. 1 shows the schematic for the treatment of BF and the preparation of corresponding FRPs. For the treatment of fiber sample, Pristine-BF was finely attached onto the edges of a ceramic boat, and then put into a CVD chamber made from a quartz tube (OTF-1200X-D4-80-SL, Hefei Kejing). The temperature of chamber was increased from room temperature to 800 ^{o}C at a heating rate 10 ^{o}C/min under a gaseous flow consisting of argon (200.0 cm^3/min) and hydrogen (14.0 cm^3/min). After keeping the sample at 800 ^{o}C for 30 min, acetylene (37.3 cm^3/min) was introduced into the system for 30 min, and Treated-BFs were obtained by cooling down the sample under argon flow (200.0 cm^3/min).

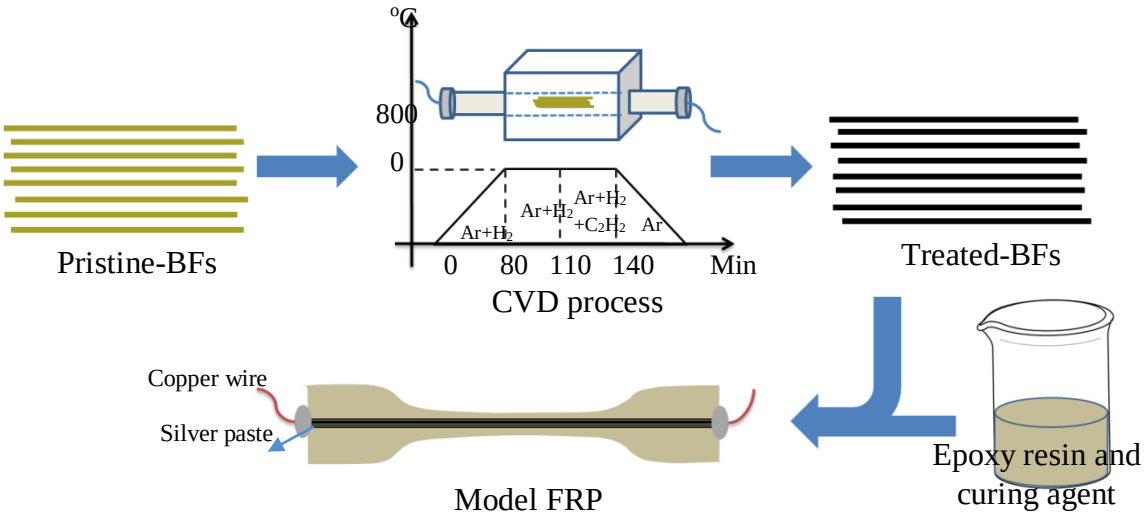

Fig. 1 Schematic illustration showing the treatment of BF using CVD process and the preparation of FRP specimen.

Model FRPs were prepared by incorporating a yarn of Treated-BF into epoxy. In a typical experiment, Treated-BF (60 mm in length) was placed in a dog-bone mold made from Teflon and the ends of yarn were connected with copper wires by silver paste. Pre-polymeric mixture consisting of epoxy

monomer (LR135) and curing agent (LH137, both from Momentive) with weight ratio of 100:35 was poured into the mold, and the sample was cured at room temperature for 24 h, followed by a post-curing at 65 ºC for 16 h.

2.2 CHARACTERIZATION

The morphology of fiber was characterized by a scanning electronic microscope (SEM, Zeiss Supra55VP). Raman spectra of samples were obtained on a Raman spectrometer with a 532 nm laser as excitation source (LabRAM-HR Evolution). The surface information of fiber was evaluated using an X-ray photoelectron spectroscopy (XPS, Thermo Escalab 250xi, Perkin Elmer). The mechanical properties of single fiber and corresponding FRPs were measured on a universal testing machine (UTM, C43-104, MTS). For single fiber test, specimens with a gauge length of 4 cm and a crosshead velocity of 0.05 cm/min were chosen for loading on the UTM equipped with a load cell of 10 N. At least 20 samples were tested and the results were analyzed using a two-parameter Weibull model [5]. The electrical resistance of single fiber was measured using a two-probe method on a digital multi-meter (34410A, Agilent). The piezoresistive properties of fiber and FRPs were evaluated by combining the results on the electrical resistance measurement with those from tensile test. For model FRPs, the in-situ resistance of sample under the load was obtained by connecting copper wires at the end of composites to the multi-meter along with a tensile rate of 0.5 cm/min on the UTM with a 10 kN load cell.

3. RESULTS AND DISCUSSION

3.1 SURFACE INFORMATION AND PROPERTIES OF BF

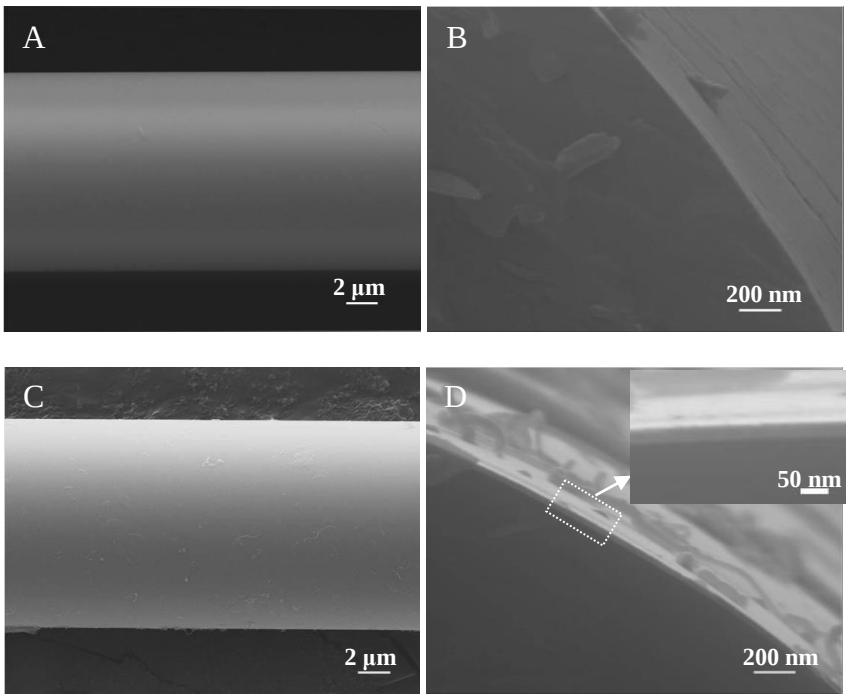

Fig. 2 SEM images showing the morphology of BF before (A and B) and after thermal treatment (C and D). The inset image in D is the enlarged area marked by dot-rectangle for showing the thickness of coating layer clearly.

Fig. 2 shows the morphology of BF before and after CVD process. Pristine-BF exhibited a smooth surface, despite of some contaminant particles on fiber surface which may be introduced during the separation of individual fiber from the yarn (**Fig. 2A**). A close examination on the fractured fiber

confirms that BF behaves a typical brittle fracture mode, and scratches on nano-meter can be observed on fiber surface (**Fig. 2B**), which were produced during the fiber production. After thermal treatment, while the surface of sample could be generally regarded as a smooth one, material with wire-like morphology was observed (**Fig. 2C**). Such structure was further confirmed by studying the cross-section of sample, and nanowires with diameter in 40 nm and length in 0.2-2 μm were attached on fiber surface (**Fig. 2D**). Our recent study confirmed that such structures originated from the growth of CNTs [13], as basalt rock contains a trace amount of ferrous/ferric ion, and it can be transformed to metallic iron (Fe) under high temperature with assistance of hydrogen, functioning as a catalyst for CNT growth.

An interesting observation was that a thin layer of coating with thickness of 15-30 nm was attached on fiber surface after thermal treatment (Inset in **Fig. 2D**). The coating could be attributed to the thermal pyrolysis of acetylene. It was reported that this compound can be decomposed to various hydrocarbons, such as CH_4, C_4H_4, H_2 as well as polycyclic aromatic hydrocarbons at high temperature [14]. The gaseous byproducts can be easily ventilated from CVD chamber under argon flow as a carrying gas, whereas the high molecular weight aromatic hydrocarbons start the nucleation process on fiber surface and initiate the aromatic condensation reactions, thus forming a polycyclic carbon coating on BF surface. The surface defects observed in Fig. 2D facilitate the formation of such coating layer.

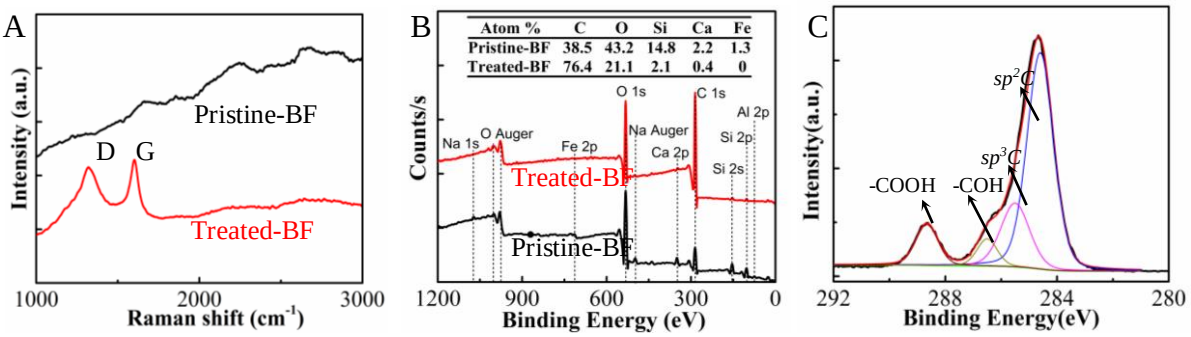

Fig. 3 Raman spectra (A), general spectra XPS (B) of Pristine-BF and Treated-BF, and C1s curve fitting of Treated-BF (C).

Raman characterization was adopted to check the surface information of fiber. From **Fig. 3A**, it can be observed that Pristine-BF showed no obvious peak due to the mixed components and disordered structure inside. As comparison, Treated-BF showed two distinct bands at ~1320 cm^{-1} and 1600 cm^{-1}. The former one is known as D-band, an indication of structural disorder in carbon-based materials, representing the breathing modes of sp^2 carbon in aromatic rings. The latter, known as G-band, is related to bond stretching of all pairs of sp^2 atoms in both rings and chains, which is usually considered as a sign of graphic structure [8]. The presence of D and G bands in the Treated-BFs confirms the coating layer was carbon-related material with graphitic structures, which was consistent with pyrolytic carbon reported in previous studies [8, 12]. Noted here that the material exhibited an intensity ratio of I_D/I_G=0.9 , possibly due to the turbo-stratic/rough laminar structure comprising low degree of graphitic textures [11]. This assumption was partly confirmed by the fact that the sample shows absence of 2D band (at around 2690 cm^{-1}), which is commonly observed in graphene samples prepared by CVD method [15], because of the intricate interaction among graphene layers in the coating.

XPS was also used to check the surface elemental composition of fibers before and after treatment. Typical composition in Pristine-BF could be considered in the form of various oxides consisting of silicon, calcium, sodium and aluminum, which are detectable based on general XPS spectra, and silicon is the highest element in the sample (**Fig. 3B**). The carbon signal in Pristine-BF may be resulted from the adventitious hydrocarbon in XPS facility. In addition, a trace amount of Fe with an

atomic ratio of Fe:O=0.03 is noted in the sample, which facilitates the direct CNT growth on BF surface without catalysts pre-deposition performed in traditional process [16], as observed in Fig. 1D. After treatment, carbon signal accounts for most of the atomic content proportion (Inset table in **Fig. 3B**), which also demonstrated the covered layer was mainly made from carbon. The chemical state of carbon in the coating was investigated by deconvoluting the C1s, as shown in **Fig. 3C**. The results on quantitative analysis showed that the coating layer was consisted of sp^2 carbon with binding energy at 284.6 eV (64.1%), sp^3 carbon at 285.5 eV (20.0%) as well as hydroxyl-contained groups like C-OH at 286.5 eV (6.0%) and -COOH at 288.6 eV (9.9%), which were generated due to the impurities and absorbing moisture from the environment [17].

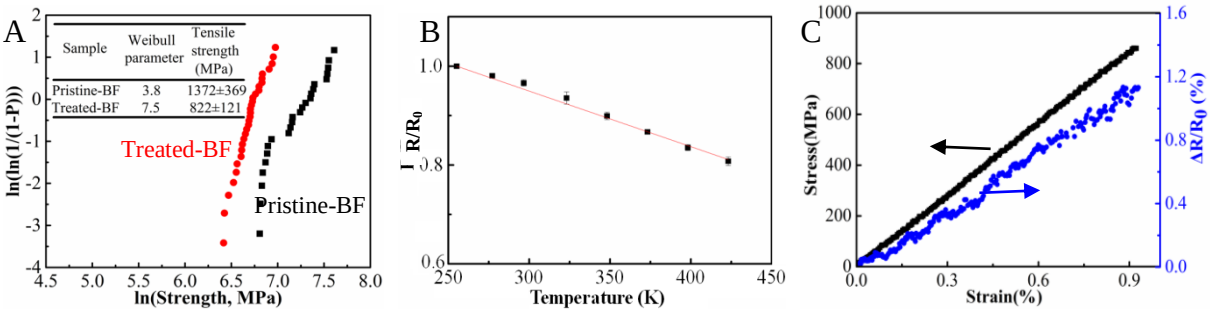

Fig. 4 Mechanical and electrical properties of fiber samples (A: Tensile properties of single fibers, where P represents the failure possibility; B: Variation on the electrical resistance of Treated-BF as a function of temperature; C: Pizeoresistive effect of Treated-BF).

The effect of heat treatment on tensile strength of fiber was shown in **Fig. 4A**. Pristine-BF showed a higher tensile strength (1372±369 MPa) than Treated-BF (822±121 MPa), which was due to the structure change in sample mainly arising from the crystallization as spinel-phase at localized areas. It is known that fibers made from basalt are initially in amorphous state, and can gradually crystallize at elevated temperatures. These transformed crystallites are more brittle and result in lower strength values [18]. As to the Weibull parameter, Treated-BF exhibited a higher value than Pristine-BF, indicating a more homogeneous distribution of surface defects on Treated-BFs due to healing effect by the carbon layer [19].

The coating led to the conversion of insulating BF to conducting one, as the measured electrical resistance R of single Treated-BF was in the range of 2.9-3.9 MΩ (4.0 cm in length). Taking a rough estimate, an average diameter of BF d=15.0 μm, thickness of coating t=22.5 nm, the specific conductivity of coating, σ, parallel to the fiber length of L, can be given by $\sigma=L/(\pi \cdot d \cdot t \cdot R)$, and the obtained electrical conductivity is in the range of 96.8-130.2 S/cm. Our extensive trial and error results showed that such high conductivity was always reachable for the coating with isotropic and homogeneous distribution on fiber surface at different positions.

The electrical resistance of single fiber was measured in the temperature range of -20-150 ºC (253-423 K). **Fig. 4B** shows the effect of temperature on the resistance (R/R_0) of sample (R_0 is the resistance at 253 K). Similar to the glass fibers with carbon nanotubes (CNTs) or graphene coating [5], Treated-BF showed a typically negative temperature coefficient (NTC) behavior, i.e., the electrical resistance of sample decreases with increasing temperature. This behavior is caused by the fact that with increasing temperature, more charge carriers of higher energy level in the coating cross the barriers between the localized states, which results in a decrease in resistance with temperature. Plotting the data in the form R/R_0 versus T gives a linear curve with a slope of -1.10×10^{-3} and a coefficient of 0.999, such high linearity indicates that the conduction in the coating layer is predominantly controlled by the transportation of carriers other than the hopping mechanism found in CNTs or graphene coating [5]

Treated-BF also displayed a typical piezoresistive effect, i.e., the electrical resistance of fiber increased linearly as a function of mechanical strain (**Fig. 4C**). The sensitivity of such behavior can be evaluated by a gauge factor $K=\Delta R/(\varepsilon R_0)=(R_\varepsilon-R_0)/(\varepsilon R_0)$, where ΔR represents the resistance change of sample, R_ε and R_0 are the resistances of sample at strain of 0% and ε, respectively. The K value for fiber sample was 0.98 in the strain range by up to 0.92%, and the good linearity of strain-$\Delta R/R_0$ curve demonstrated that the resistance change of sample was dominated by the variation on the contacting resistance and tunneling effect among the graphene-like particles in the coating under the slight deformation [20].

3.2 PIEZORESISTANCE OF FRPs

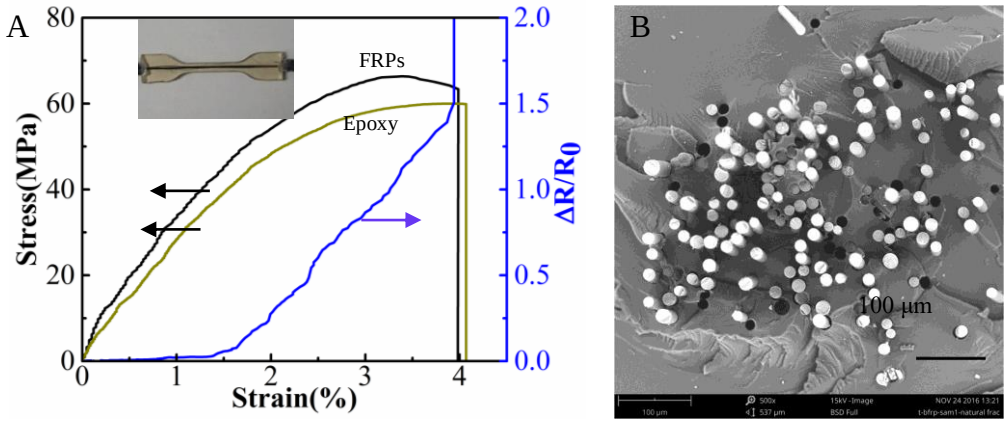

Fig. 5 Piezoresistive response (A) and fractured surface (B and C) of FRPs reinforced by Treated-BF.

To evaluate the feasibility of Treated-BF for monitoring health state in FRPs, composites with a bundle of fibers embedded in epoxy were prepared (Inset in Fig. 4A) and the piezoresistance of material under the tensile condition was studied. It is reasonable that the prepared FRPs displayed a higher tensile strength (66.7±9.5 MPa) than that of pure epoxy (60.3±2.2 MPa) due to the reinforcement of basalt fibers. However, such enhancement was marginal because of the low volume fraction of fibers in FRPs (Calculated V_{fiber}<1.0%). In sharp contrast, the resistance of composites varied significantly under different tensile strain, and three stages were observed, as shown in **Fig. 5A**: I) When the strain increased from 0 to 1.4%, the resistance of sample increased from 356 to 366 kΩ with a gauge factor of 2.0, suggesting negligible deformation of conducting networks in composites under small strain; II) When the strain varied in the range of 1.4%-3.9%, the resistance of composites increased drastically by 2.4 times (from 366 to 892 kΩ), and the gauge factor was 38.6 at the strain of 3.9%, just before the total failure of composites. More importantly, the resistance change ($\Delta R/R_0$)-strain curve showed an interesting "tilted-steps", indicating one after another failure of individually conductive fibers in composites. It should be noted here that the resistance increased gradually from a lower step to the higher one, differing from the suddenly jumping behavior in FRPs reinforced by fibers with CNT and graphene coatings [6]. This difference could be explained based on the interfacial dissimilarities between the matrix and coated fibers by CNT or graphene [5]. Interphase in the former case would be the formation of polymer-based nanocomposites reinforced by CNTs, resulting in a abrupt failure of conducting networks in FRPs, whereas the one with graphene coating mainly consisted of multi-layer structures, which could sustain a stable conducting network under the high deformation due to the interlayer sliding of graphene. III) With a strain higher than 3.9%, the electrical resistance of composite jumped to the infinity, indicating the breakage of conductive fibers in the sample. It should be noted here that this behavior happened at the strain of 3.9%, earlier than the fractured strain of matrix (4.1%) and FRPs (4.0%). This behavior along with the piezoresistive response of sample observed in Stage II suggests that the Treated-BF can be used for the early warning of damage in FRP structures.

The fractured morphology of FRPs was examined by SEM (**Fig. 5B**). It is clear that the polymer matrix can penetrate into the fiber bundle, resulting in the separation of individual reinforcement with each other and uniform fiber distribution in matrix, which facilitates the one by one breakage of fibers under mechanical loading, corresponding to the phenomena observed in Stage II in **Fig. 5A**. The interphase between the fiber and matrix was visualized by a close examination on the fractured surface (**Fig. 5C**). As expected, the fibers were pull-out in most cases, suggesting the poor interfacial interactions between the fiber and matrix, which further confirm the resistance change of FRPs under strain originated from the failure of individual conductive BFs.

4. CONCLUSIONS

Treatment of BFs with CVD process generated a thin layer of pyrolytic carbon coating with thickness around 20 nm onto fiber surface. The coating mainly consisted of sp^2 carbon, and the inherently conducting nature of carbon makes insulating basalt fiber conductive with a negative temperature coefficient behavior. Additionally, the coating led to the basalt fiber exhibited a piezoresistive effect under strain with a gauge factor of 0.98. Model FRPs were prepared by employing Treated-BFs as filler and epoxy as polymer matrix. The results on the mechanical and electrical properties of composites showed that Treated-BFs not only increased the tensile strength of material, but also could detect structure failure inside the sample as reflected by the resistance change. In the strain from 1.4% to 3.9%, the resistance of FRP sample increased drastically in a "tilted steps" way with the highest gauge factor of 39. This behavior demonstrated the damage accumulation by one after another failure mode of conductive fibers in FRPs, suggesting the Treated-BFs displayed huge potential to be a sensor to monitor structural damage.

ACKNOWLEDGEMENTS

This project was supported by the National Natural Science Foundation of China (Project No. 11472294), and the 1000-Talent Program (Recruitment Program of Global Expert, In Chinese: Qian-Ren-Ji-Hua). Part of research was conducted when Bin Hao and Peng-Cheng Ma were supported by the China-Germany Scientific Cooperation Program (PPP, Grant No. 2014-6065).

REFERENCES

[1] Hafsa J, Rajesh M. A green material from rock: basalt fiber - a review. J Textile Institute 2016, 107, 923-937.
[2] Tábi T, Égerházi AZ, Tamás P, Czigány T, Kovács JG. Investigation of injection moulded poly(lactic acid) reinforced with long basalt fibres. Compos A, 2014, 64, 99-106.
[3] Bhat T, Chevali V, Liu X, Feih S, Mouritz AP. Fire structural resistance of basalt fibre composite. Compos A. 2015, 71: 107-115.
[4] J. Sim, C. Park, D.Y. Moon, Characteristics of basalt fiber as a strengthening material for concrete structures, Composites Part B-Engineering 36 (6-7) (2005) 504-512.
[5] B. Hao, Q. Ma, S. Yang, E. Mäder, P.-C. Ma, Comparative study on monitoring structural damage in fiber-reinforced polymers using glass fibers with carbon nanotubes and graphene coating, Compos. Sci. Technol. 129 (2016) 38-45.
[6] J. Rausch, E. Maeder, Health monitoring in continuous glass fibre reinforced thermoplastics: Tailored sensitivity and cyclic loading of CNT-based interphase sensors, Compos. Sci. Technol. 70 (13) (2010) 2023-2030.
[7] L. Liu, P.C. Ma, M. Xu, S.U. Khan, J.K. Kim, Strain-sensitive Raman spectroscopy and electrical resistance of carbon nanotube-coated glass fibre sensors, Compos. Sci. Technol. 72 (13) (2012) 1548-1555.
[8] C.A. Taylor, W.K.S. Chiu, Characterization of CVD carbon films for hermetic optical fiber coatings, Surf. Coat. Technol. 168 (1) (2003) 1-11.

[9] D.-h. Ding, W.-c. Zhou, F. Luo, D.-m. Zhu, Influence of pyrolytic carbon coatings on complex permittivity and microwave absorbing properties of Al_2O_3 fiber woven fabrics, Transactions of Nonferrous Metals Society of China 22 (2) (2012) 354-359.
[10] H. Yu, X. Zhou, W. Zhang, H. Peng, C. Zhang, Mechanical behavior of SiCf/SiC composites with alternating PyC/SiC multilayer interphases, Materials & Design 44 (2013) 320-324.
[11] F. Cancino-Trejo, M. Sáenz Padilla, E. López-Honorato, U. Carvajal-Nunez, J. Boshoven, J. Somers, The effect of heat treatment on the microstructure and diffusion of silver in pyrolytic carbon coatings, Carbon 109 (2016) 542-551.
[12] S.-T. Shiue, P.-Y. Chen, R.-H. Lee, T.-S. Chen, H.-Y. Lin, Effects of deposition parameters on characteristics of carbon coatings on optical fibers prepared by thermal chemical vapor deposition, Surf. Coat. Technol. 205 (3) (2010) 780-786.
[13] T. Förster, B. Hao, E. Mäder, F. Simon, E. Wölfel, P.-C. Ma, CVD-Grown CNTs on basalt fiber surfaces for multifunctional composite interphases, Fibers 4 (4) (2016) 28.
[14] K. Norinaga, V.M. Janardhanan, O. Deutschmann, Detailed chemical kinetic modeling of pyrolysis of ethylene, acetylene, and propylene at 1073–1373 K with a plug-flow reactor model, Int. J. Chem. Kinet. 40 (4) (2008) 199-208.
[15] V. Ivan, S. Sergei, I. Ilia, F.F. Pasquale, D. Sheng, M. Harry, et al., Electrical and thermal conductivity of low temperature CVD graphene: the effect of disorder, Nanotechnology 22 (27) (2011) 275716.
[16] H. Qian, A. Bismarck, E.S. Greenhalgh, G. Kalinka, M.S.P. Shaffer, Hierarchical composites reinforced with carbon nanotube grafted fibers: The potential assessed at the single fiber level, Chem. Mater. 20 (5) (2008) 1862-1869.
[17] A. Siokou, F. Ravani, S. Karakalos, O. Frank, M. Kalbac, C. Galiotis, Surface refinement and electronic properties of graphene layers grown on copper substrate: An XPS, UPS and EELS study, Appl. Surf. Sci. 257 (23) (2011) 9785-9790.
[18] S.M.M. Sabet, F. Akhlaghi, R. Eslami-Farsani, The effect of thermal treatment on tensile properties of basalt fibers, Journal of Ceramic Science and Technology 6 (3) (2015) 245-248.
[19] P.C. Ma, J.W. Liu, S.L. Gao, E. Mäder, Development of functional glass fibres with nanocomposite coating: A comparative study, Compos A 44 (2013) 16-22.
[20] L.M. Chiacchiarelli, M. Rallini, M. Monti, D. Puglia, J.M. Kenny, L. Torre, The role of irreversible and reversible phenomena in the piezoresistive behavior of graphene epoxy nanocomposites applied to structural health monitoring, Compos. Sci. Technol. 80 (17) (2013) 73-79.